Investigation Of An AMB Based Auxiliary Mass Dynamic Absorber

L. Scott Stephens, Assistant Professor
Sankaran Jagadeesh, Research Assistant

2508 CEBA Bldg., Department of Mechanical Engineering
Louisiana State University, Baton Rouge, Louisiana, 70803-6413, USA
Phone: (504) 388-5905; Fax: (504) 388-5924; e-mail: stephens@me.lsu.edu

Abstract: This paper investigates the effectiveness of a magnetic bearing when used as an auxiliary mass dynamic absorber. The system is modeled as a 2-DOF, lumped mass approximation with a linearized actuation force. The accuracy of force linearization for an AMB absorber is discussed. Performance of the absorber is quantified on the basis of response attenuation, required actuating force and robustness to uncertainty in the actuating force. Performance is assessed under constrained PD control and robust μ-synthesized control approximated by DK iteration. Results indicate that magnetic bearings are plausible in such an application when implemented with higher order μ-synthesized control.

1 Introduction

Figure 1 shows the general 2-DOF auxiliary mass dynamic absorber consisting of a main system with mass, M, stiffness, K_1, and damping c_1, an auxiliary mass, m, and a control force, F_c. The objective of such an absorber is to attenuate the response of the main mass, x_1, to the input disturbance, d, by using the control force which actuates against the inertia of the auxiliary mass.

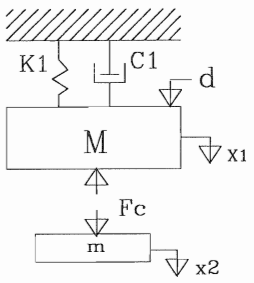

Figure 1: General Auxiliary Mass Dynamic Absorber

The actuator which generates the control force can take the form of mechanical elements such as springs and dampers [1], [3], [5]. The actuator may also take the form of an actively controlled device such as a piezoelectric actuator [6] [7] or a magnetic actuator as investigated in this paper. The former configuration being termed passive control and the latter being termed active control [4].

Previous work in the area of passive control includes that of Den Hartog [5], who optimized the performance of the absorber using a single spring and damper pair as the control elements (such an arrangement is equivalent to ideal PD control). Under this form of control, for mass ratios, m/M, less than about 1/3, exceptional main mass response attenuation resulted at the cost of large relative displacement between the auxiliary and main masses. Such large relative displacements cause prohibitively large stresses in the mechanical control elements, making it difficult to implement such absorbers, practically. However, it was shown that for mass ratios greater than about 1/3, excellent response attenuation can be achieved with significantly smaller relative displacements.

Previous work in the area of active control includes that of Rouch[7], who proposed the use of a piezoelectric actuator as the control element. In general, active control elements were found to be limited in stroke and force generating capability, essentially limiting the allowable relative displacement and reducing the effectiveness of PD control, even at larger mass ratios. Rouch was able to show the added effectiveness of higher order control by successfully implementing a deterministic LQR state-feedback control. The main benefit of the piezoelectric actuator in such a control scheme being high linearity, resulting in a well-known force displacement relationship.

This paper investigates the use of a magnetic bearing as the control element in the auxiliary mass dynamic absorber. Issues including force-displacement-current non-linearity and relative displacement constraints due to the air gap are discussed. Response attenuation and required actuating force are assessed for the absorber under constrained PD and robust μ-synthesized control.

2 System Modeling

For implementation of an AMB as the actuator in an absorber, the system model must include the radial air gaps and the differential nature of the actuator. Figure 2 shows the schematic of the 2-DOF dynamic AMB based absorber with the auxiliary mass constrained to move internally to the main system by the gaps, g_t and g_b. Differential magnetic forces, F_t and F_b, act on the top and bottom of the auxiliary mass, respectively. Such forces can be generated via a magnetic bearing constructed of two opposing horseshoe magnets. In such a configuration, the magnetic bearing "journal" is part of the auxiliary mass, and the magnetic bearing "stator" is part of the main system. The control

element in the absorber is then the magnetic force between the two masses, and the gaps g_t and g_b, are the bearing air gaps at the top and bottom magnets, respectively.

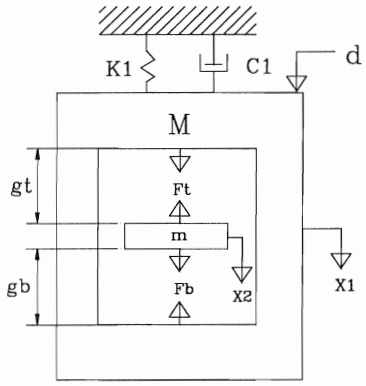

Figure 2: Model of An AMB Based Absorber

The equations of motion for the absorber can be derived via Newton's method and are given as:

$$M\ddot{x}_1 + c_1\dot{x}_1 + K_1x_1 = F_t - F_b + d \quad (1)$$

$$m\ddot{x}_2 = F_b - F_t \quad (2)$$

where all variables have been previously defined. Note that the motion of the system is constrained by the bearing air gaps. The instantaneous air gaps are related to the displacements by:

$$g_t = g_0 - (x_1 - x_2) \quad (3)$$

$$g_b = g_0 + (x_1 - x_2) \quad (4)$$

where g_o is the nominal air gap. Assuming the input disturbance is harmonic and considering only the *forced* system response, the constraint imposed by the air gaps can be written in terms of the frequency response of the relative displacement. Physically, each instantaneous air gap must be greater than zero. However, for magnetic bearings, the constraint is more restrictive as it is known that system instability and loss of performance occurs for large relative displacement. The constraint can then be written as:

$$\max_{\omega} |X_r(\omega)| < \beta g_o \quad (5)$$

where, X_r is the relative displacement and β is in the range $0<\beta<1$, which specifies the relative displacement to be some fraction of the nominal air gap.

The top and bottom magnet forces can be combined into a single actuation force given below.

$$F_{act} = F_t - F_b \quad (6)$$

Finally, the force-current-displacement relationship for the actuator force is approximated by the following equation:

$$F_{act} = \mu_o AN^2 \left[\frac{I_t^2}{g_t^2} - \frac{I_b^2}{g_b^2} \right] \quad (7)$$

where μ_o is the permeability of free space, A is the cross sectional area of the magnet poles, N is the number of turns of wire in each magnet coil and I_t and I_b are the total current in the top and bottom magnets respectively. Note that this force is nonlinear with applied current and relative displacement (in addition to eddy currents and hysteresis). Recall that previous results using unconstrained ideal PD control required a significant amount of relative displacement to attenuate response of the main mass.

From the above development, there are two main challenges for the simplified AMB based absorber:

- attenuating the main mass response in spite of the limit on relative displacement imposed by the air gap constraint;
- designing systems in which main mass attenuation is robust to the nonlinear actuating force.

To determine the feasibility of overcoming these challenges, the approach taken is to linearize the actuator force and to use robust control methods to overcome the uncertainty of the actuator force. The actuator force can be linearized by dividing the current in the top and bottom magnets into a bias current, I_B, and a differential perturbation current, $\mp I_p$, respectively. A multivariable Taylor's series expansion about the perturbation current and the auxiliary mass centered position, linearizes the actuation force as:

$$F_{act} = F_{act}|_0 - \left.\frac{\partial F_{act}}{\partial x_1}\right|_0 x_1 - \left.\frac{\partial F_{act}}{\partial x_2}\right|_0 x_2 - \left.\frac{\partial F_{act}}{\partial I_p}\right|_0 I_p + HOT \quad (8)$$

where HOT are the higher order terms and are neglected. Finally, the linearized actuation force is given by:

$$F_{act} = -K_p(x_1 - x_2) + K_i I_p \quad (9)$$

where,

$$K_p = \frac{-4\mu_0 AN^2 I_B^2}{g_0^3}, \quad K_i = \frac{4\mu_o AN^2 I_B}{g_o^2} \quad (10)$$

and where K_p and K_i are the bearing negative stiffness and current gain, respectively. Substituting eq. (9) into eqs. (1) and (2), defining a set of state variables as $\mathbf{z} = [x_1,\ x_1 - x_2,\ \dot{x}_1,\ \dot{x}_1 - \dot{x}_2]'$, and using the main mass and relative displacements as the measured states, a state-space representation of the system is derived and given below.

$$\dot{\mathbf{z}} = A\mathbf{z} + \mathrm{B_F}d + \mathrm{B_c}I_p \quad (11)$$

$$\mathbf{y} = C\mathbf{z} \quad (12)$$

$$A = \begin{bmatrix} 0 & 0 & 1 & 0 \\ 0 & 0 & 0 & 1 \\ \frac{-K_1}{M} & -\frac{K_p}{M} & \frac{-c_1}{M} & 0 \\ \frac{-K_1}{M} & -K_p\left(\frac{1}{M}+\frac{1}{m}\right) & \frac{-c_1}{M} & 0 \end{bmatrix} \quad (13)$$

$$B_f = \begin{bmatrix} 0 \\ 0 \\ \frac{1}{M} \\ \frac{1}{M} \end{bmatrix}, \quad B_c = \begin{bmatrix} 0 \\ 0 \\ \frac{K_i}{M} \\ Ki\left[\frac{1}{M}+\frac{1}{m}\right] \end{bmatrix} \tag{14}$$

$$C = \begin{bmatrix} 1 & 0 & 0 & 0 \\ 0 & 1 & 0 & 0 \end{bmatrix} \tag{15}$$

Note that no sensor noise is included in the model as this paper focuses upon the uncertainty in the actuator with relative displacement.

Assuming that the harmonic disturbance, d, has amplitude P_o, the low frequency or *static* displacement of the main mass can be expressed as:

$$X_{st} = \frac{P_o}{K_1} \tag{16}$$

where X_{st} is static displacement of the main mass. Using eq. (16), the frequency response of the absorber can be expressed in terms of the main mass and relative displacement amplification factors:

$$\frac{X_1}{X_{st}} = \frac{X_1}{P_o}(K_1), \quad \frac{X_r}{X_{st}} = \frac{(X_1 - X_2)}{P_o}(K_1) \tag{17}$$

where the upper case letters indicate frequency domain quantities. Attenuation results are presented in terms of these amplification factors, which is consistent with previous work in this area.

3 Control Formulation

3.1 Control Objectives

The control objectives for the absorber are: (1) to levitate the auxiliary mass relative to the main mass (stability); (2) to attenuate the main mass response while satisfying the relative displacement constraint; and (3) to attenuate the main mass response in spite of the uncertain actuator force. To meet these objectives constrained PD and robust μ-synthesized control are implemented and compared.

3.2 Constrained, Ideal PD Control

The PD control law takes the form:

$$I_p = a(x_1 - x_2) + b(\dot{x}_1 - \dot{x}_2) \tag{18}$$

where a and b are the proportional and derivative feedback gains. In order to incorporate the constraint of eq. (5) into controller synthesis, the following dimensionless parameters are defined:

$$\alpha = \frac{X_{st}}{g_o}, \quad \beta = \frac{\overline{X}_r}{g_o} \qquad \begin{matrix} (0 < \alpha < \infty) \\ (0 < \beta < 1) \end{matrix} \tag{19}$$

where $\overline{X}_r$ is the maximum *allowable* relative displacement over frequency. The parameter α can be seen as a load parameter which models the effect of the low frequency component of the applied force, P_o, by comparing the resulting static displacement to the nominal air gap. As before, the parameter β specifies the fraction of the air gap in which the auxiliary mass is allowed to move. Note that the ratio β/α specifies the allowable X_r / X_{st} for the absorber. As the results will show, performance of the absorber under PD control is determined by this ratio alone. However, for the purposes of including the air gap constraint in terms of the static displacement in the problem, the parameters α and β are used.

Under ideal PD control, and given the polarity of the perturbation currents, stability of the system is guaranteed if the following relationships are satisfied:

$$-K_p + aK_i < 0, \quad b < 0 \tag{20}$$

therefore, for the closed loop system, the optimal constrained PD control gains can be found by solving the constrained optimization problem given below.

$$\min_{a<\frac{K_p}{K_i},\, b<0} \left[\max_{\omega} \left| \frac{X_1(\omega)}{X_{st}} \right| \right] \quad \forall \max_{\omega} \left| \frac{X_r(\omega)}{X_{st}} \right| < \frac{\beta}{\alpha} \tag{21}$$

3.3 Robust, μ-Synthesized Control

The basis of robust control is accurately modeling the system uncertainty using perturbations on the nominal model, and synthesizing controllers which perform in spite of the uncertainty. Complex perturbations, denoted $\Delta(j\omega)$, are norm-bounded using the transfer function ∞-norm,

$$\|\Delta(j\omega)\|_\infty = \sup_{\omega} \bar{\sigma}[\Delta(j\omega)] \tag{22}$$

and are normalized by stable minimum phase frequency dependent weighting functions, $W(j\omega)$. The weighting functions are appended to the system model such that $\|\Delta\|_\infty \le 1$ represents the range of uncertainty or a specified performance in the system.

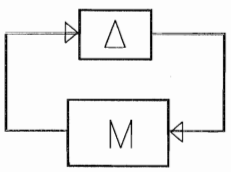

Figure 3: General Perturbation Representation

Perturbation locations are preserved during controller design by using the *structured singular value*, μ, as a measure of the closed loop stability and performance. Considering Figure 3, the structured singular value of closed loop system $M \in C^{nxn}$, for complex perturbations $\Delta \in C^{nxn}$, is defined as:

$$\mu(M) := \frac{1}{\min\left(\overline{\sigma}(\Delta) : \det(I - M\Delta) = 0\right)} \tag{23}$$

where Δ is a member of the block diagonal set $\underline{\Delta}$. Computation of the structured singular value using eq. (23) is intractable, but bounds on μ can be computed for complex perturbations using the following relations [2]:

$$\max_{\Gamma \in \underline{\Gamma}} \rho(\Gamma M) \le \mu(M) \le \inf_{D \in \underline{D}} (DMD^{-1}) \tag{24}$$

where, among others, D is any real, diagonal, positive matrix with a certain block diagonal structure. In general, Δ has the block structure $\Delta = [\Delta_p, 0; 0, \Delta_u]$ where Δ_u is the uncertainty and Δ_p represents the performance specifications for the system. If M has the corresponding structure $M = [M_{11} M_{12}; M_{21} M_{22}]$, then the following stability and performance tests result:

$$\mu_\Delta(M_{22}) < 1 \quad \textit{Nominal Performance} \tag{25}$$

$$\mu_\Delta(M_{11}) < 1 \quad \textit{Robust Stability} \tag{26}$$

$$\mu_\Delta(M) < 1 \quad \textit{Robust Performance} \tag{27}$$

where nominal performance is specified performance of the nominal plant, robust stability is stability of all uncertain plants, and robust performance is specified performance of all uncertain plants.

Design of controllers in a μ framework is accomplished using the DK iteration method which approximates μ-synthesis. Figure 4 illustrates the open loop interconnection structure for DK iteration, where, **m**, are the measurements, **c** is the control input, **u** and **q** are the uncertainty inputs and outputs and **d** and **v** are the performance inputs and outputs.

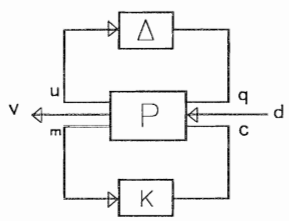

Figure 4: Open Loop Interconnection Structure

Since the upper bound for μ in eq. (24) may be obtained by scaling and applying $\|\bullet\|_\infty$, DK iteration proceeds by finding a stabilizing H_∞ controller, K, and a scaling matrix, D, such that the following minimization occurs:

$$\min_{D \in \underline{D}, K} \left\| DF_l(P,K)D^{-1} \right\|_\infty \tag{28}$$

where $F_l(P,K)$ is the lower linear fractional transformation between the open loop interconnection, P, and the stabilizing controller, K [2]. For the AMB absorber, $F_l(P,K)$ is the complimentary sensitivity between the main mass and relative displacements and the input disturbance.

Figure 5 shows the AMB absorber open loop interconnection structure with all weights and perturbations appended to the nominal plant $G_{nom}(s) = [A, B; C, D]$.

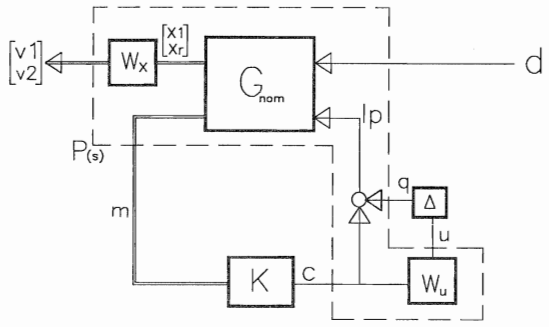

Figure 5: Open Loop Interconnection Structure For The AMB Absorber, μ-Synthesized Control

A performance weight is augmented to the system of the form $W_x(s) = [w_{x1}(s), 0; 0, w_{xr}(s)]$. This weight specifies performance on the closed loop complementary sensitivity, T_{xd}, between the main mass and relative displacements and the input disturbance. In words, the performance specification is to attenuate the main mass response as much as possible given a specified amount of relative displacement. Using eqs. (16) and (19), the following limit on the relative displacement can be defined.

$$\frac{\overline{X_r}}{P_o} = \frac{\beta K_1}{\alpha} \tag{29}$$

Giving this specification a frequency shaping, the weighting functions, are given as:

$$w_{x1}(s) = \frac{\alpha}{\beta} \frac{10}{K_1} \frac{(s+1000)}{(s+10{,}000)}, \quad w_{xr}(s) = \frac{w_{x1}(s)}{2} \tag{30}$$

where $w_{x1}^{-1}(s)$ and $w_{xr}^{-1}(s)$ are the specified upper bound on the responses of the main mass and relative displacements, respectively.

Finally, an input multiplicative uncertainty models the uncertainty in the actuator force by specifying a multivariable gain margin at the actuator. A multivariable gain margin of 1.3 is specified by selecting an uncertainty weight of $W_u = 0.3$. Assuming robust performance is achievable, this allows a +/-30% range on the nominal actuator force before loss of performance or stability.

4 Results

Results are presented for PD and μ-synthesized control of the AMB absorber with a mass ratio of m/M=0.5, a main mass natural frequency of 252 rad/sec, a spring constant of $K_1 = 2944$ lb/in, main mass damping ratio of 0.4% and a negative stiffness and current gain of -10,000 lb/in and 12 lb/amp, respectively. A mass ratio of 0.5 was selected because previous results indicated good main mass attenuation with relatively small relative displacement for PD control.

4.1 Constrained PD Control: General Solutions

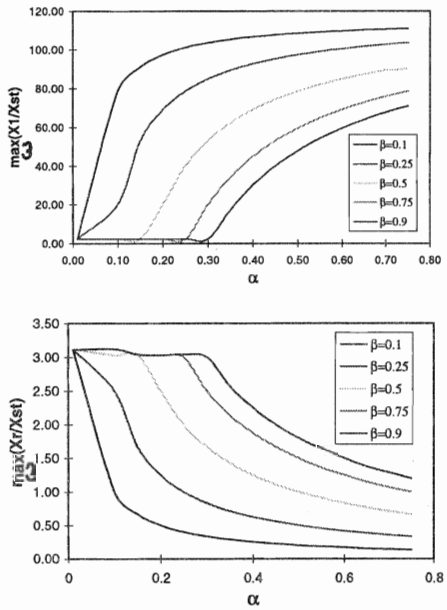

Figure 6: Amplification Factors; (a) Main Mass (b) Relative

Figure 6a shows the effectiveness of PD control in attenuating the main mass response as a function of α and β for the nominal system. Figure 6b shows the resulting maximum relative displacement. Note there is a region where no further attenuation occurs regardless of the allowable relative displacement. At this point the problem becomes unconstrained and the global optimum is obtained.

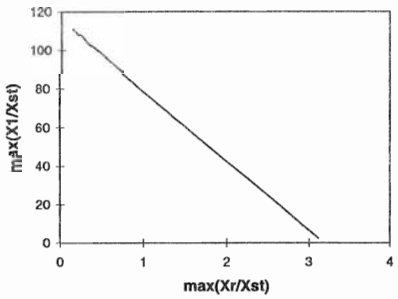

Figure 7: Main Mass Response Attenuation, Dependence Upon Relative Displacement Under PD Control

Figure 7 shows the main mass attenuation as a function of the maximum allowable relative displacement. As previously mentioned, all of the curves in Figure 6 reduce to the curve in Figure 7. It is seen than that the maximum allowable relative displacement exclusively determines the main mass attenuation under PD control. However, Figures 6a and 6b are useful in interpreting the results in the context of the AMB air gap. For instance, for a nominal radial air gap of 0.010", several illustrative cases may be constructed from the data of Figures 6a and 6b using eqs. (16) and (19).

Table 1: Nominal Performance For Different α and β Values for An Air Gap of 0.010"

	Case 1	Case 2	Case 3	Case 4
β	0.25	0.25	0.90	0.90
α	0.75	0.10	0.75	0.30
$\overline{P_o}$	22.1	2.9	22.1	8.8
$\max_{\omega}\left\lvert\frac{X_1}{X_{st}}\right\rvert$	105	19	70.0	2.2
$\max_{\omega}\left\lvert\frac{X_r}{X_{st}}\right\rvert$	0.25	2.5	1.40	3.0
No Absorber	110	110	110	110

Table 1 shows four such cases which include maximum force accommodation, $\overline{P_o}$, for cases 1 and 3, and maximum main mass attenuation for cases 2 and 4, for values of β=0.25 and β=0.9. Also shown is the maximum amplification factor, X_1/X_{st}, for the main mass displacement with *no absorber*, for comparison. Given the non-linearity of the actuator with increasing β, the case of β=0.25 is more appropriate for magnetic bearings.

The results indicate that the constrained AMB absorber is only effective in the lightly loaded region (small α). Note that these results say nothing about robustness of the PD controlled system to the uncertain actuating force.

4.2 PD and μ: Nominal Performance

A comparison of system performance between PD and μ-synthesized control is made for all absorbers with β/α=0.3. For PD control, the constrained optimal gains were found to be a=-886.9 and b=-0.241. Figure 8a shows the resulting amplification factors for this case under PD control. Figure 8b shows the same for the nominal system under μ-synthesized control. Also shown in Figure 8b are the upper bound on the amplification factors as specified in the performance weight.

Figures 8a and 8b indicate that in the nominal case, the μ-synthesized controller attenuates the main mass response twice as much as the PD control for the same amount of relative displacement. In both control cases, the required maximum actuating force per unit disturbance amplitude was $F_{act} / P_o = 10.8\ lb$. This presents another challenge for

magnetic bearings in this application due to their relatively low specific load capacity.

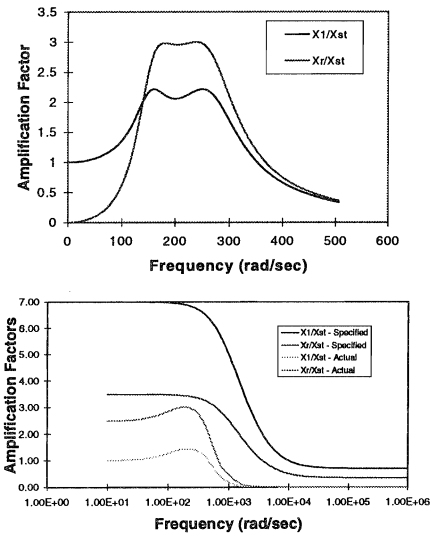

Figure 8: (a) Response for β/α=3.0, PD Control, (b) Response for β/α=3.0, μ Control

4.3 PD and μ: Robust Performance

Robust performance of the system under the μ-synthesized control was achieved for the specified weights as μ=1.01 resulted from the robust performance test of eq. (27). The resulting H_∞ controller has 14 states where the plant order is only 4, illustrating the tradeoff of higher order control.

One key question is how the closed loop system behaves under each type of control for variations in the actuator force. In an attempt to quantify this, the effect on system stability and performance of variations, δ_p and δ_i, in K_p and K_i, respectively, were investigated.

Referring to Table 2, stability and performance for the nominal system with $\delta_p = 0$, $\delta_i = 0$ is shown for comparison. For the case of PD control, stability under the variations is easily determined using eq. (20). The maximum variation is 6.4% independently or 3.1% in opposite directions, simultaneously, before the PD controlled system becomes unstable. Note the performance and stability of the μ controlled system is unaffected even up to variations as high as 30% simultaneously. Further investigation yields that the μ controlled system remains stable for simultaneous variations up to 35%. This correlates well with the specified multivariable gain margin of 30% used in the design.

These results show that μ-synthesized controllers can achieve good response attenuation even with a constrained relative displacement over a large variation in actuator force. However, it is seen that PD control loses stability for small uncertainties in the actuator force. These results encourage further work in this area.

Table 2: Robust Stability and Performance

Var. (%)		Stab.		Perf. X_1/X_{st}		Perf. X_r/X_{st}		Force F_{act}/P_o	
δ_p (+)	δ_i (-)	PD	μ	PD	μ	PD	μ	PD	μ
0	0	s	s	2.2	1.45	3.0	3.0	10.8	10.9
6.4	0	u	s	-	1.45	-	3.0	-	10.9
0	6.4	u	s	-	1.45	-	3.0	-	10.9
3.1	3.1	u	s	-	1.45	-	3.0	-	10.9
30	0	u	s	-	1.43	-	3.01	-	13.9
0	30	u	s	-	1.42	-	3.02	-	10.9
30	30	u	s	-	1.39	-	3.03	-	13.9

5 Conclusions

The purpose of this paper was to investigate the feasibility of implementing a magnetic bearing as the actuator in an auxiliary mass dynamic absorber. Several conclusions can be drawn from the results: (1) maintaining stability would be very difficult under PD control due to poor robustness to the actuator force non-linearity; (2) good main mass attenuation is achievable under μ-synthesized control and is robust to the force non-linearity, and (3) a large actuation force is required to accommodate the disturbance, which represents an additional challenge for magnetic bearing in this application. The results encourage more investigation into this new application for magnetic bearings.

References

[1] Brock J.E ," A Note on the Damped Vibration Absorber ", *Journal of Applied Mechanics, Vol.68,* p. A-284, 1946

[2] Doyle, J., "Analysis of Feedback Systems with Structured Uncertainties", *IEE Proceedings,* v. 120, part D, n. 6, November 1982, pp. 242-250

[3] Ema S. and Marui E.," A Fundamental Study On Impact Dampers", *International J. on Machine Tools Manufacturing, Vol 34, pp 407-421,1994*

[4] Herzog R., "A Comparison between Passively and Actively Controlled Magnetic Bearings, *3rd Intl. Symp. on Magnetic Bearings, pp.* 223-231,1992

[5] Ormondroyd J. and Den Hartog J.P.," The Theory of the Dynamic Vibration Absorber ,*"Transactions of ASME,* 7, pp. 9-22, 1921

[6] Stephens L .S., Rouch K.E. and Tewani S.G.," Theory For An Active Dynamic Vibration Absorber", *Proceedings of the ASME 13th Biennial Conference on Mechanical Vibration and Noise*, Miami, FL, pp. 89-94,1991

[7] Tewani S .G. ,Rouch K.E. and Walcott L. B., "Active Vibration Control Using Dynamic Absorber", *Proceedings of IEEE International Conference on Robotics and Automation,* Sacramento, CA, 1991